

# Analyst

Accepted Manuscript



This is an *Accepted Manuscript*, which has been through the Royal Society of Chemistry peer review process and has been accepted for publication.

*Accepted Manuscripts* are published online shortly after acceptance, before technical editing, formatting and proof reading. Using this free service, authors can make their results available to the community, in citable form, before we publish the edited article. We will replace this *Accepted Manuscript* with the edited and formatted *Advance Article* as soon as it is available.

You can find more information about *Accepted Manuscripts* in the [Information for Authors](#).

Please note that technical editing may introduce minor changes to the text and/or graphics, which may alter content. The journal's standard [Terms & Conditions](#) and the [Ethical guidelines](#) still apply. In no event shall the Royal Society of Chemistry be held responsible for any errors or omissions in this *Accepted Manuscript* or any consequences arising from the use of any information it contains.

# Efficient Microfluidic Negative Enrichment of Circulating Tumor Cells in Blood using Roughened PDMS

*L. Diéguez<sup>a†</sup>, M. A. Winter<sup>a†</sup>, K. J. Pockock<sup>a</sup>, K. E. Bremmell<sup>b</sup> and B. Thierry<sup>a</sup>*

Cite this: DOI: 10.1039/x0xx00000x

Received 00th January 2012,  
Accepted 00th January 2012

DOI: 10.1039/x0xx00000x

www.rsc.org/

Efficient isolation strategies not based on epithelial biomarker expression are required to enable non-biased enrichment of circulating tumor cells (CTCs). CTCs undergoing epithelial-mesenchymal transition (EMT) may be prognostically relevant, and importantly are not detected with conventional epithelial based approaches such as CellSearch®. A method for the non-biased isolation of cancer cells within a peripheral blood sample utilizing microfluidic mixing PDMS devices functionalized with anti-CD45 is reported. The introduction of micro and nanoscale roughness using a single step treatment with sulfuric acid significantly increases the binding yield of white blood cells (WBCs) to the anti-CD45 conjugated surfaces. Up to 99.99% WBC depletion is achieved with a tumor cell recovery yield of 50%. This high level of CTC enrichment is expected to facilitate the detailed characterization of CTCs using for instance, imaging flow cytometry as demonstrated here.

## Introduction

Detection and enumeration of circulating tumor cells (CTCs) in patient blood has been established as a prognostic biomarker in many types of cancer.<sup>1, 2</sup> Despite a very large body of academic work in the last 5 years, the CellSearch® System by Veridex LLC remains to date the only CTC detection technique with FDA approval. This method isolates and identifies CTCs through their expression of epithelial markers including EpCAM and cytokeratin. The use of microfluidic devices for the isolation of CTCs (i.e. positive enrichment) has rapidly advanced over the past decade, and many techniques have been developed following on the pioneering work by Nagrath et al which effectively isolated the cancer cells based on their epithelial phenotype i.e. EpCAM.<sup>3-5</sup> However, identification of prognostically important cancer cells in patients' blood is not limited to those which express epithelial markers. Epithelial Mesenchymal Transition (EMT), is a process whereby cancer cells lose their epithelial characteristics and gain a mesenchymal phenotype.<sup>6</sup> CTCs that are able to undergo EMT are more likely to metastasise and may be associated with poorer patient prognosis.<sup>7</sup> Importantly, CTC detection techniques which rely solely on epithelial marker expression will not detect this potentially prognostically relevant mesenchymal cellular population.<sup>6</sup> For this reason, CTC detection methods which do not rely solely on the presence of epithelial markers are currently being actively developed.<sup>8</sup> These include physical based technologies including selection based on size,<sup>9, 10</sup> density and electrical charge based separation<sup>11</sup> and negative enrichment.<sup>12-15</sup>

Negative enrichment describes the selective removal of cells not of interest from a sample, therefore, enriching the collection of cells of

potential interest. Negative enrichment is typically achieved using magnetic beads immuno-conjugated to target a specific antigen on the cell membrane of the non-target cells.<sup>14</sup> For CTC isolation, the main approach is aimed at the depletion of white blood cells (WBC) which are specifically targeted using antibodies against the leucocyte common antigen (CD45). Building on the excellent performance of microfluidic devices in isolating CTCs, a microfluidic approach has been recently reported for negative enrichment.<sup>16</sup> Using an anti-CD45 functionalized device, a negative enrichment yield of close to 99% was obtained using Jurkat cells as a model for WBC. CTCs could be successfully enriched from the blood of cancer patients although the residual quantity of WBCs, which is expected to be more challenging considering the heterogeneity of CD45 expression, was not presented in this study.

Towards further improving on the negative enrichment yields afforded by microfluidic approaches, here we report on a simple method to introduce nano/microscale roughness on PDMS devices to enhance the binding of WBC to anti-CD45 functionalized devices (**Figure 1**). Nanostructured substrates have been demonstrated to significantly increase binding yields of tumor cells<sup>17, 18</sup> and we demonstrate here that the binding yield of WBC directly correlated with the water contact angle of roughened PDMS. Building on the excellent level of negative enrichment achieved here, we also demonstrate the compatibility of the proposed negative microfluidic enrichment approach with imaging flow cytometry. The combination of efficient negative enrichment with the unique features of imaging flow cytometry is expected to provide a reliable method to elucidate the phenotypical changes associated to haematological dissemination of tumor cells and potentially improve patient prognosis and/or direct treatment.

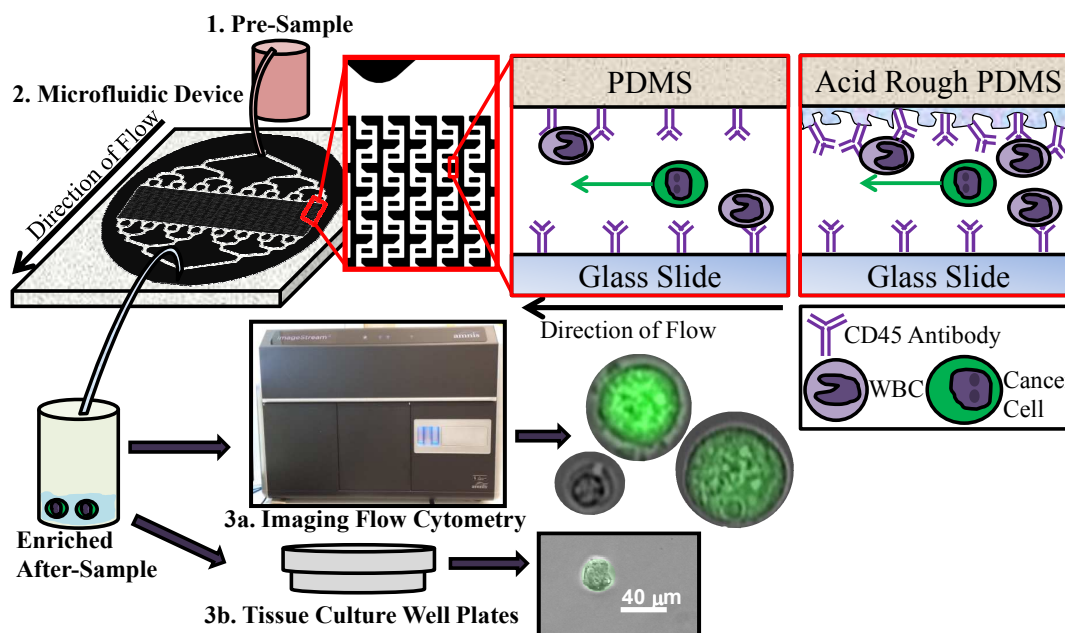


**Figure 1.** Schematic representation of the experimental design: (1,2) blood pre-samples with spiked cancer cells are injected through the depletion device functionalized with anti-CD45 antibody to specifically bind to white blood cells (WBCs). Eluted cells comprising the target CD45<sup>-</sup> cells and false positive WBCs are collected and characterized using either imaging flow cytometry (3a) or optical microscopy after plating in standard tissue culture wells (3b).

## Results and Discussion

### Optimization of experimental conditions

The anti-CD45 functionalized devices were fabricated using standard soft lithography. The design was selected to enhance mixing of the sample inside the devices. It consists in a highly parallelized array of micro-channel favouring chaotic mixing of the flowing medium (Figure 1). The mixing channels have lengths of 1.6 cm, widths of 80  $\mu\text{m}$  and heights of 150  $\mu\text{m}$ . We first investigated the effect of the flow rate on the depletion of WBC from whole blood. Flow rates of 2, 12 and 20  $\mu\text{l}/\text{min}$  were chosen which correspond to linear velocities of 40, 240 and 400  $\mu\text{m}/\text{s}$  respectively. We found that the WBC depletion efficiency was highly flow rate dependent and the maximum depletion was obtained at a flow rate of 2  $\mu\text{l}/\text{min}$  (Figure 2A), which is in good agreement with literature<sup>19-21</sup>. It is noteworthy that the actual blood flow could be easily increased while maintaining the depletion yield through multiplexing in the device or modifying its dimensions, the device we used here was used to demonstrate the feasibility of this approach.

The WBC depletion percentage in whole blood remained, however, quite low at 87.0% (Figure 2A). We hypothesized that this was due to the presence of RBCs physically hindering WBC binding within the device. Therefore, to minimise the number of cellular components and steric hindrances standard RBC lysis was used. We then compared the depletion efficiency of lysed blood to whole blood and found that the use of lysed blood resulted in a much

greater WBC depletion percentage than whole blood (98.6% compared to 87.0%) (Figure 2B). Further experiments were therefore performed with lysed blood which should in no way impact cell characteristics.

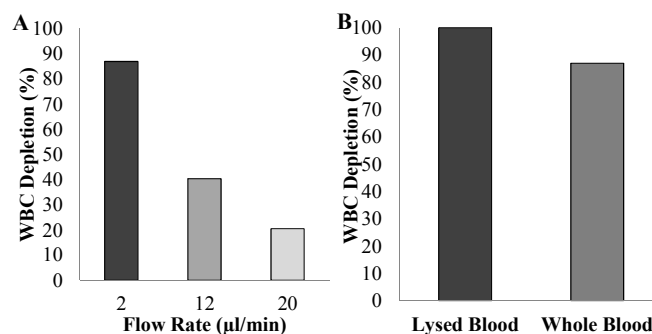


**Figure 2.** A) White blood cell (WBC) depletion of whole blood (%) of the sample passing through the CD45 microfluidic negative enrichment device at varying flow rates ( $\mu\text{l}/\text{min}$ ). B) WBC depletion (%) of the sample after exiting microfluidic device using either whole peripheral blood or lysed peripheral blood from healthy donors.

### Effect of PDMS roughening on CD45 immunocapture of WBC

High immuno-binding yields on substrates with nanoscale roughness have been reported and nanorough substrates such as etched silicon and glass have been successfully used to isolate CTCs using antigens

Analyst

specific to tumor cells.<sup>18</sup> To the best of our knowledge the use of nanorough devices for negative enrichment procedure has not previously been investigated and we hypothesize here that the use of PDMS with nanoroughness could further increase the binding of WBCs within the device after functionalization with anti-CD45 antibodies. To this end, we extended on the simple yet efficient approach described by de Givenchy et al which relies on a single treatment with concentrated sulfuric acid to etch PDMS and create micro and nano-scale features.<sup>22</sup> The static contact angle with water, used here as an indirect measurement of the roughness, readily increased with the sulfuric acid time and plateaued at 30 sec (**Figure 3**). The roughened PDMS samples were then functionalized with an anti-CD45 antibody and the WBC binding yields in a static assay were determined. As shown in Figure 3, the amount of WBCs bound to the surface correlated to the contact angle, confirming the positive effect of increased roughness on the WBC binding yield. To further investigate the effect of the acid treatment and confirm the increased roughnesses of the treated samples, atomic force microscopy (AFM) imaging was conducted. As shown in **Figure 4** and **Table 1**, acid treated samples were significantly rougher ( $R_a$  of 0.4 nm for untreated sample vs. 101 nm and 202 nm for the 20 sec and 60 sec treated sample respectively) than the untreated ones. The AFM data was in good agreement with the contact angle measurements, and confirmed that maximal roughness is achieved within approximately 30 sec of acid treatment.

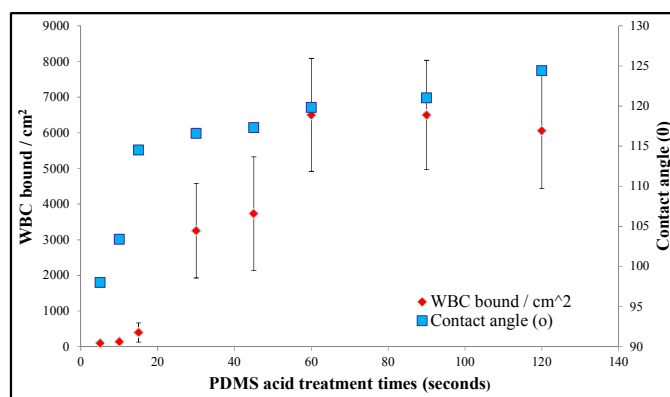


**Figure 3.** Correlation between the number of white blood cell (WBCs; red diamond) bound to nanoroughened PDMS, the contact angle of PDMS (Blue square) and the duration of acid treatment.

**Table 1.** Roughness of the PDMS samples measured with the AFM. (The roughness reported here is the average of two measurements from different sample positions; in the brackets is the standard deviation)

Sample	$R_a$ (nm)
Untreated PDMS	0.4 (0.004)
20 seconds	101.4 (12.2)
60 seconds	202.5 (21.0)
2 minutes	203.5 (38.9)

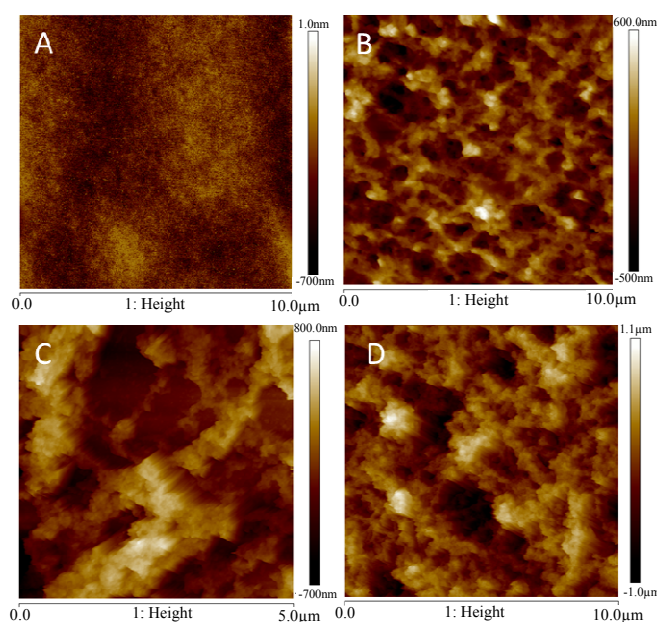


**Figure 4.** AFM height images of the PDMS samples; A) untreated, and treated for B) 20 seconds, C) 60 seconds and D) 2 minutes

#### Optimization of WBC depletion in roughened PDMS devices

In order to assess the ability for the acid roughening to increase the binding affinity of CD45+ cells and therefore, WBC depletion, the acid treatment was adapted to the microfluidic devices. Sulfuric acid was injected inside the PDMS devices and a treatment time of approximately 30 sec was used (caution: extreme care should be taken to avoid splash in case of device failure). In good agreement with the data obtained on planar specimen, the acid roughening increased the WBC depletion percentage when compared to non-roughened device from 98.6 to 99.9% respectively (**Figure 5A**). Considering the very high level of depletion obtained with the roughened devices, the use of concentrated samples was investigated next in order to increase the amount of sample analysed. As can be seen in **Figure 5B** in the acid roughened devices, high WBC depletion percentages were maintained with increasing concentrations of lysed blood (99.93, 99.99, 99.77, 99.74% for 1 $\times$ , 2 $\times$ , 4 $\times$  and 8 $\times$ , respectively). It was also noted that at all concentrations there was further capacity for WBC binding within the device and that most of the binding as expected occurred at the start of the device, this was particularly evident in the acid roughened devices which appears to display a greater affinity (**Figure 5C and D**). However, at higher equivalent blood concentrations (i.e. 8 $\times$ ), device clogging became an issue, and thus in these devices the concentration factor is limited. Occasional clogging of channels could result in the loss of the target tumor cells. Therefore, the optimum cellular concentration for WBC depletion in the current design is 4 $\times$  concentrated than normal healthy blood.



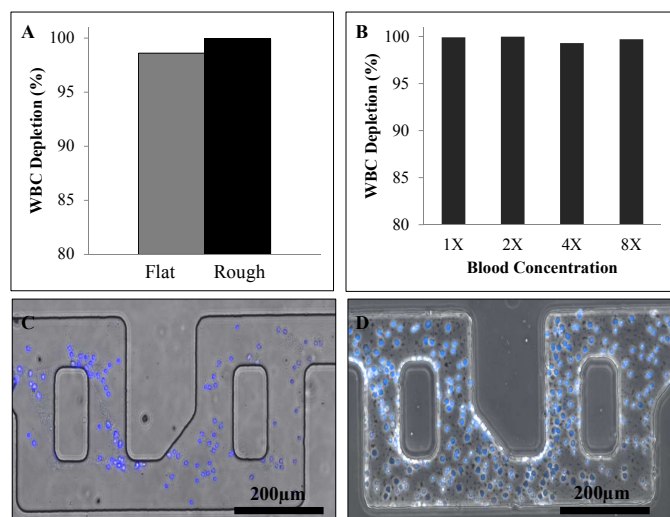


**Figure 5.** White blood cell (WBC) depletion of a 1× concentrated lysed blood sample and the effect of non-acid treated flat (light grey bar) and acid treated rough (dark grey bar) microfluidic depletion devices (A). WBC depletion of varying concentrations of lysed blood in acid treated rough microfluidic depletion devices (B). Photomicrographs of WBCs bound in the middle sections of serpentine microfluidic depletion devices: non-acid treated device (C) and acid treated device (D) (10× magnification, scale bar 200μm).

Finally we benchmarked the proposed microfluidic negative enrichment approach with the commercially available RosetteSep™ assay (STEMCELL™). This assay is based on a tetramer antibody which binds both WBCs and RBCs and then allows efficient separation of cancer cells with density centrifugation. In our laboratory we achieved depletion level of 99.96% with this assay, in good agreement with the technical specification.<sup>23</sup> In direct comparison to the proposed approach, the RosetteSep method has a slightly lower WBC depletion percentage and therefore would result in an increased number of contaminating cells. A WBC depletion of 99.99% as achieved with our device at 2× concentration would indeed result in approximately 1000 WBCs contaminating the CTC sample for every mL of blood analysed (assuming approx.  $5 \times 10^6$  WBC/ml). On the other hand, a WBC depletion of 99.96% as achieved with the RosetteSep would result in approximately 4000 contaminating WBC. These differences would become even more pronounced when analysing the standard volume of 7.5ml of cancer patient blood. In addition, compared to the level of WBC depletion of other negative enrichment technologies (Table 2), including Hyun and colleagues microfluidic negative enrichment and standard immuno-magnetic methods, the microfluidic method yielded an excellent depletion percentage (99.99 vs. 98.94 and 99.81 vs. 99.98 respectively). Ultimately, the required level of WBC depletion is inherently linked to the downstream analytical methodology. Lower numbers of false-positive WBCs facilitate immunohistochemical investigations. On the other hand, molecular methods currently used to phenotype/genotype CTCs such as RT-PCR or next generation sequencing require high levels of purities in order to conduct pooled analysis. In addition, a recent significant development in cancer research has been the shift towards single cell analysis. The latter can be conducted either through manual “selection” of the target cells, or using (semi)automated platforms such as the C1 chip from Fluidigm. In general the lower the number of the contaminating blood cells the more simple and reliable the subsequent analysis.

**Table 2.** Comparison of the white blood cell (WBC) depletion and cancer cell recovery of the acid roughened microfluidic negative enrichment device with other techniques reported in literature.

	WBC Depletion	Cancer Cell Recovery
Acid roughened microfluidic negative enrichment device	99.99%	~50%
Hyun and colleagues microfluidic negative enrichment device <sup>16</sup>	98.94%	42.10-94.67%
RosetteSep	99.96% <sup>a)</sup>	~60% <sup>24</sup>
Immuno-magnetic Beads <sup>13,14</sup>	99.81-99.98%	~60-80%
<sup>a)</sup> In good agreement with technical specifications <sup>23</sup>		

#### Tumor cell recovery yield and downstream analysis with imaging flow cytometry

After optimisation of WBC depletion the yield of recovery of breast cancer cells spiked into healthy blood was determined (Figure 1 and 6). Recovery rates of 50% of the MCF-7 cells (experiment was performed in duplicate) were observed when approximately 180 cancer cells were spiked. This is comparable with the previously published microfluidic negative enrichment approach which achieved a recovery of MCF-7 cells from 94.67% with 50 spiked cancer cells down to 42.10% with 1000 spiked cancer cells in  $10^6$  leukocytes (Table 2).<sup>16</sup> When compared to the recovery rates of negative enrichment approaches based on immuno-magnetic beads, which typically range between 60 to 80%<sup>13</sup> microfluidic approaches appear to slightly under perform. Loss of CTCs in microfluidic devices can be due either to their non-specific binding to the rough surface or to their entrapment into small cellular clusters with WBC. The latter is a common issue to all immuno-depletion methods and could limit their clinical relevance considering the growing recognition of the importance of cellular clusters containing CTCs.<sup>25</sup>

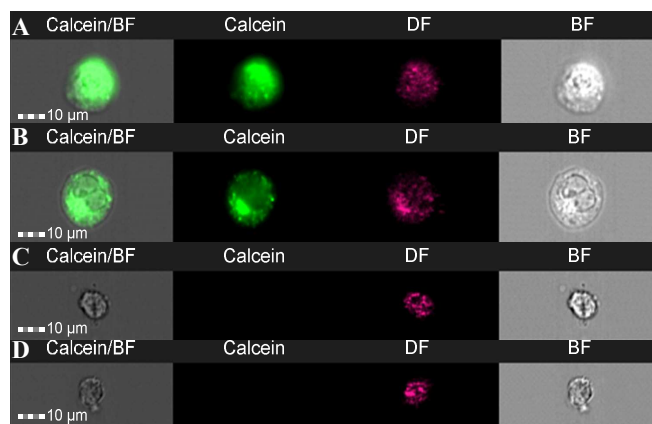


**Figure 6.** Microscope images at 40× magnification of individual cells and their fluorescence profile from imaging flow cytometry. As labelled left to right the composite image (incorporates a brightfield and calcein), Calcein (live stain used to stain cancer cells before spiking), Darkfield (DF) and Brightfield (BF). Images have been adjusted to enhance visual appearance. A,B) Calcein stained MCF-7 cells, C,D) WBCs showing no calcein staining.

Based on the principle of positive enrichment of CTCs using magnetic beads, the CellSearch system has a cancer cell recovery

greater than 80%. However, the latter is achieved only for tumor cells with high expression of epithelial markers<sup>26</sup>. The CellSearch system is therefore intrinsically limited through its inability to detect circulating tumor cells that have undergone EMT and thus no longer or weakly express epithelial markers which are likely to hold prognostic significance. On the other hand, the unbiased nature of negative enrichment means that the recovery of CTCs is independent of their phenotypes, and therefore, is a significant feature towards establishing the prognostic value of CTCs, especially in regards to EMT. Association between the presence of CTCs with mesenchymal phenotypes in the blood of breast cancer patients with disease progression was recently observed.<sup>27</sup>

This study demonstrates that microfluidic WBC depletion is a promising alternative to enrich CTCs and therefore, facilitate their downstream detection and characterization using molecular or immunological technologies. Of particular interest is the use of imaging flow cytometry which bridges the gap between traditional flow cytometry and microscopy. Tumor cells eluted from the negative enrichment device could be readily imaged using an imaging flow cytometer (Figure 1 and 6). Besides providing a powerful way to characterize the phenotype of CTCs, imaging flow cytometry can also enable detailed cytomorphological analysis. This feature could provide further patient prognostic indications.<sup>28, 29</sup> Imaging flow cytometry allows for analysis of many morphological parameters including circularity, elongation, cellular area and nuclear features including nucleus to cytoplasm ratio.

## Experimental

### Materials

3" silicon wafers were purchased from Micro Materials & Research Cons. Pty Ltd (Australia), SU-8 50 photoresist was purchased from MicroChem (USA) and Polydimethylsiloxane (PDMS) elastomer SYLGARD 184 was purchased from Dow Corning (USA). 75cm<sup>2</sup> tissue culture dishes were purchased from Sarstedt, Nümbrecht (Germany). (3-Glycidyloxypropyl)trimethoxysilane (GPTMS), trichloro 1,1,2,2-perfluorooctyl-silane, (3-aminopropyl)trimethoxysilane (APTMS), glutaraldehyde (GA), phosphate buffered saline (PBS), formaldehyde, Triton™ X-100, Trypsin/EDTA, DMEM, Fetal Bovine Serum, Penicillin/Streptomycin, Calcein, ammonium chloride (NH<sub>4</sub>Cl), Potassium bicarbonate (KHCO<sub>3</sub>), Ethylenediaminetetraacetic acid (EDTA) and 4',6-Diamidino-2-phenylindole dihydrochloride (DAPI) were purchased from Sigma Aldrich (USA). Specific monoclonal antibody CD45 clone HI30 was purchased from Biologend (USA). All other chemicals were analytical grade. MCF-7 breast adenocarcinoma cell line was obtained from ATCC (USA). Peripheral blood samples were collected from healthy donors in compliance with the University of South Australia Human Research Ethics Committee. The syringe pumps (model KDS-212-CE, KDS-210) used were obtained from KD Scientific.

### Fabrication of microfluidic devices

Masters for PDMS moulding were fabricated using standard photolithography techniques. Silicon wafers were cleaned by subsequent sonication steps in acetone and isopropanol for 5 minutes each, dried with nitrogen and activated in oxygen plasma for 5 minutes. Upon activation the wafers were immersed in 5% GPTMS in ethanol for 1h, rinsed in ethanol and cured at 80°C for 1 hour.

SU8-50 was dispensed on the wafer, which was then accelerated at 250 rpm to 500 rpm for 5 seconds, and further to 1600 rpm at 500 rpm for 30 seconds. The wafer was soft baked in 2 steps, first at 65°C for 10 minutes and secondly at 95°C for 30 minutes. The wafer

was then exposed through a transparency mask (JD tools) with a UV lamp with a dose of 250 mJ/cm<sup>2</sup> and postbaked at 55°C overnight. The sample was developed during 20 minutes and hardbaked ramping from 65°C to 200°C.

Prior to master replication, the wafer was hydrophobized with a vapour-phase treatment in trichloro 1,1,2,2-perfluorooctyl-silane for 1 hour in a desiccator and cured for another hour at 80°C. PDMS was mixed at 1:10 ratio, degassed, poured over the master, degassed again and cured at 80°C for 2 hours. After curing, the PDMS was unmolded and inlet and outlet were punched. Finally, clean glass slides and PDMS replicas were treated with oxygen plasma at low power for 15 seconds and subsequently brought in contact to produce irreversible bonding.

### Acid roughening of PDMS and microfluidic devices

Flat pieces of PDMS were air plasma treated for 30 seconds, then 95-97% sulfuric acid was loaded directly onto the PDMS surface for varying amounts of time (5, 10, 15, 30, 45, 60, 90 and 120 seconds) promptly rinsed in water and subsequently soaked in isopropanol for 2 minutes and finally left to dry. After roughening, for cell binding experiments PDMS was functionalised using the same protocol as for the microfluidic devices. The level of roughening achieved in the PDMS surface was assessed by measuring its hydrophobicity by means of contact angle and using the tangent method. To acid treat microfluidic devices, devices were manually filled with ethanol using a syringe, then washed with MilliQ water and then 95-97% sulfuric acid was quickly pushed into the device (Extreme caution must be exercised to avoid splash of sulfuric acid from failing devices). Longer acid treatments (greater than 30 seconds) can result in device breakage, therefore, as soon as acid entered the chamber devices were washed with water.

### Atomic Force Microscopy analysis of roughness

Roughness of the PDMS samples were determined from height AFM images acquired using the Multimode 8 (Bruker, USA) placed on an active anti-vibration table (Vision IsoStation, Newport, USA), equipped with a vertical engagement scanner "J". The AFM images were collected in ScanAsyst mode in air. Silicon nitride cantilevers with a resonance frequency between 50 and 90 kHz, a spring constant of 0.4 N/m, and a sharp silicon tip (SCANASYST-AIR, Bruker, USA) were used. All images were taken at high (512 x 512) resolution. Scan rates employed in imaging were 0.8 Hz or lower. The roughness reported is the arithmetic mean roughness (Ra) calculated from a 10 µm image. (Ra is the arithmetic average of the absolute values of the surface height derivations measured from the mean plane.)

### Functionalization of the microfluidic devices

Upon activation with oxygen plasma, the microfluidic devices were connected to a syringe pump and filled with ethanol. All the functionalization steps were carried out at 100 µl/min. After stabilization in ethanol, 2% APTES in ethanol was withdrawn into the device for 30 minutes and rinsed in ethanol for 10 minutes. Then the buffer was changed to MilliQ water and stabilized for 10 minutes prior to withdrawing 1% glutaraldehyde in water for another 30 minutes and rinsing in water for 10 minutes. Sterile PBS was then withdrawn into the device and equilibrated for 10 minutes just before introducing 200 µl of 50 µg/ml CD45 in PBS that was left to react overnight at 4°C. Unreacted antibody was then rinsed with PBS for 10 minutes and the surface blocked with 2% BSA in PBS.

### Cell culture and sample preparation

The human breast adenocarcinoma cell line MCF-7 was used in this study to mimic patient CTC and mixed with whole or lysed

peripheral blood. MCF-7 breast cancer cells were cultured in 75cm<sup>2</sup> tissue culture dishes in DMEM supplemented with fetal bovine serum and penicillin/streptomycin at 37°C, 5% CO<sub>2</sub> in a humidified environment. MCF-7 were detached from culture flasks with trypsin/EDTA (Sigma Aldrich, St. Louis, MO., USA) prior to use and stained with calcein (Sigma Aldrich, St. Louis, MO., USA) to enable accurate detection of the enrichment yields. MCF-7 cells were resuspended in DMEM at appropriate concentration for use in blood spiking i.e. 10,000 cells/ml. Peripheral blood was collected from healthy volunteers (in compliance with the University of South Australia Human Research Ethics Committee) into an EDTA vacutainer, and used within 5 hours after collection. For lysed blood samples, whole blood was lysed using the following buffer 145mM NH<sub>4</sub>Cl, 10mM KHCO<sub>3</sub>, 0.1mM EDTA in MilliQ water (Sigma Aldrich, St. Louis, MO., USA), in a 25:1 dilution buffer:blood for 10 minutes. White blood cells were then collected following centrifugation and diluted in MCF-7 cancer cell solution. After RBC lysis, either 1× (0.5ml of whole blood resuspended in 0.5ml PBS), 2× (1ml of whole blood resuspended in 0.5ml PBS), 4× (2ml whole blood resuspended in 0.5ml PBS) or 8× (4ml whole blood resuspended in 0.5ml PBS) blood concentration factor solutions were made. At least 200 µl of blood sample was used for each sample.

### Negative enrichment in roughened PDMS devices

Cellular solutions were injected through the anti-CD45 functionalized microfluidic devices using syringe pumps. Typically, 200 µl of the cell solution was processed through the device to allow for reliable quantitative measurements. Cell numbers (WBC and MCF-7) were determined using imaging flow cytometry (Image Stream X, AMNIS, Seattle, WA, USA) prior to the start of each experiment. The sample recovered from the negative enrichment microfluidic device was either analysed with imaging flow cytometry or plated onto a tissue culture dish for microscopic observation (Figure 1). For the latter, the cells were allowed to adhere overnight before fixation with formalin. Tissue culture dishes were also thoroughly examined for the presence of white blood cells or MCF-7 cancer cells. Microscopy was carried out using a Nikon Ti Eclipse inverted fluorescence microscope. Microfluidic devices were also systematically examined for the presence of cancer cells (as indicated by calcein staining). Cells were also stained with DAPI (nuclear stain).

### Imaging flow cytometry studies

To demonstrate the compatibility of the microfluidic negative enrichment approach with downstream high throughput molecular and morphological characterization, the sample recovered from the devices was analysed with the state-of-the-art Imaging Flow Cytometer Image Stream X. All cells were stained with DAPI excited with the 405 laser in channel 1 of the ISX. Channel 2 and the 488 laser recorded calcein positive events while, channel 4 and 6 were set for brightfield and darkfield images, respectively. A cell classifier of 50 µm<sup>2</sup> area was applied in order to eliminate small debris and speed beads (AMNIS, Seattle, WA, USA).

### Conclusions

A non-epithelial based non-biased CTC isolation strategy is urgently required so that the correct number of patient CTCs in blood can be enumerated, especially those with mesenchymal phenotypes which are broadly expected to be associated with poorer prognosis. We have shown in this proof of principle study that microfluidic negative enrichment technology is very efficient at depleting WBCs from a blood sample, particularly when combined with a nanorough surface to increase cellular binding. The use of nanorough surfaces

efficiently increases the cell binding and therefore volume of blood sample that can be analyzed with one device. PDMS devices fabricated using standard methodology could be easily and reliably roughened using a single treatment step with sulfuric acid. We have also demonstrated that imaging flow cytometry is a powerful technology for the detection, enumeration and characterization of circulating tumor cells. This technology can provide both phenotypic and morphological information about these rare cancer cells and can potentially provide a greater patient prognosis.

The overall depletion efficiency (>99.7%) and tumor cell recovery yield (~50%) using the proposed approach is among the highest reported to date, which is expected to facilitate the detailed characterization of CTCs using for instance imaging flow cytometry. High enrichment yields and therefore purity are especially important towards advanced molecular and phenotypical characterization using technologies with less contamination tolerance such as next generation sequencing. Such microfluidic negative depletion technology could provide a suitable companion isolation technology, eliminating the need for complex micromanipulation of the cellular targets. Further development and up-scaling of the device are required before such a technique would become clinically viable. The analysis of a large volume of blood (>10 mL) is indeed desirable to reliably isolate cancer cells in patients with a very low CTC number. Ultimately this technology could become valuable providing high purity samples and allowing advanced molecular characterization of cancer cell populations potentially improving patient prognosis and/or direct treatment.

### Acknowledgements

This work was supported by the NSW Cancer Council and the NHMRC Project grant APP1045841. B. Thierry is supported by a NHMRC CDA Fellowship. This work was performed in part at the South Australian node of the Australian National Fabrication Facility, a company established under the National Collaborative Research Infrastructure Strategy to provide nano and micro-fabrication facilities for Australia's researchers. Author 1 and 2 contributed equally to this work.

### Notes and references

<sup>a</sup> Ian Wark Research Institute, University of South Australia, Mawson Lakes Campus, SA 5095, Australia.

<sup>b</sup> School of Pharmacy and Medical Sciences, University of South Australia, City East Campus, North Terrace, Adelaide, SA 5000, Australia

† Co-first Authors

1. M. G. Krebs, R. L. Metcalf, L. Carter, G. Brady, F. H. Blackhall and C. Dive, *Nature Reviews Clinical Oncology*, 2014, **11**, 129-144.
2. F.-C. Bidard, D. J. Peeters, T. Fehm, F. Nolé, R. Gisbert-Criado, D. Mavroudis, S. Grisanti, D. Generali, J. A. Garcia-Saenz and J. Stebbing, *The lancet oncology*, 2014, **15**, 406-414.
3. S. Nagrath, L. V. Sequist, S. Maheswaran, D. W. Bell, D. Irimia, L. Ulkus, M. R. Smith, E. L. Kwak, S. Digumarthy and A. Muzikansky, *Nature*, 2007, **450**, 1235-1239.
4. S. L. Stott, C.-H. Hsu, D. I. Tsukrov, M. Yu, D. T. Miyamoto, B. A. Waltman, S. M. Rothenberg, A. M. Shah, M. E. Smas and G. K. Korir, *Proceedings of the National Academy of Sciences*, 2010, **107**, 18392-18397.
5. K.-A. Hyun and H.-I. Jung, *Lab Chip*, 2013, **14**, 45-56.
6. S. Kasimir-Bauer, O. Hoffmann, D. Wallwiener, R. Kimmig and T. Fehm, *Breast Cancer Research*, 2012, **14**, R15.
7. G. Barriere, A. Riouallon, J. Renaudie and M. Tartary, *BMC cancer*, 2012, **12**, 114-125.
8. C. Alix-Panabières and K. Pantel, *Clinical chemistry*, 2013, **59**, 110-118.



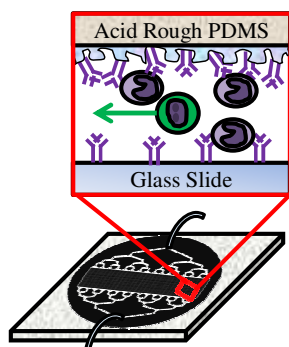
## Analyst

- 1  
2  
3  
4  
5  
6  
7  
8  
9  
10  
11  
12  
13  
14  
15  
16  
17  
18  
19  
20  
21  
22  
23  
24  
25  
26  
27  
28  
29  
30  
31  
32  
33  
34  
35  
36  
37  
38  
39  
40  
41  
42  
43  
44  
45  
46  
47  
48  
49  
50  
51  
52  
53  
54  
55  
56  
57  
58  
59  
60
9. S. Zheng, H. K. Lin, B. Lu, A. Williams, R. Datar, R. J. Cote and Y.-C. Tai, *Biomedical microdevices*, 2011, **13**, 203-213.
10. H. K. Lin, S. Zheng, A. J. Williams, M. Balic, S. Groshen, H. I. Scher, M. Fleisher, W. Stadler, R. H. Datar and Y.-C. Tai, *Clinical Cancer Research*, 2010, **16**, 5011-5018.
11. C. Huang, H. Liu, N. H. Bander and B. J. Kirby, *Biomedical Microdevices*, 2013, **15**, 941-948.
12. P. Balasubramanian, J. C. Lang, K. R. Jatana, B. Miller, E. Ozer, M. Old, D. E. Schuller, A. Agrawal, T. N. Teknos and T. A. Summers, *PloS one*, 2012, **7**, e42048.
13. Z. Liu, A. Fusi, E. Klopocki, A. Schmittl, I. Tinhofer, A. Nonnenmacher and U. Keilholz, *Journal of translational medicine*, 2011, **9**, 70.
14. L. Yang, J. C. Lang, P. Balasubramanian, K. R. Jatana, D. Schuller, A. Agrawal, M. Zborowski and J. J. Chalmers, *Biotechnology and bioengineering*, 2009, **102**, 521-534.
15. M. Lustberg, K. R. Jatana, M. Zborowski and J. J. Chalmers, *Recent results in cancer research*, 2012, **195**, 97-110.
16. K.-A. Hyun, T. Y. Lee and H.-I. Jung, *Analytical chemistry*, 2013, **85**, 4439-4445.
17. S. Wang, K. Liu, J. Liu, Z. T. F. Yu, X. Xu, L. Zhao, T. Lee, E. K. Lee, J. Reiss and Y. K. Lee, *Angewandte Chemie International Edition*, 2011, **50**, 3084-3088.
18. L. Wang, W. Asghar, U. Demirci and Y. Wan, *Nano Today*, 2013.
19. A. Sin, S. K. Murthy, A. Revzin, R. G. Tompkins and M. Toner, *Biotechnology and bioengineering*, 2005, **91**, 816-826.
20. D. S. Kim, S. H. Lee, T. H. Kwon and C. H. Ahn, *Lab on a Chip*, 2005, **5**, 739-747.
21. Y. Wan, J. Tan, W. Asghar, Y.-t. Kim, Y. Liu and S. M. Iqbal, *The Journal of Physical Chemistry B*, 2011, **115**, 13891-13896.
22. E. T. de Givenchy, S. Amigoni, C. Martin, G. Andrada, L. Caillier, S. G eribaldi and F. Guittard, *Langmuir*, 2009, **25**, 6448-6453.
23. Stemcell Technologies, RosetteSep™ Human Circulating Epithelial Tumor Cell Enrichment Cocktail. <http://www.stemcell.com/en/Products/Popular-Product-Lines/RosetteSep/Tumor-Cell-Enrichment-Cocktail.aspx>, accessed:September 2014
24. W. He, S. A. Kularatne, K. R. Kalli, F. G. Prendergast, R. J. Amato, G. G. Klee, L. C. Hartmann and P. S. Low, *International Journal of Cancer*, 2008, **123**, 1968-1973.
25. N. Aceto, A. Bardia, D. T. Miyamoto, M. C. Donaldson, B. S. Wittner, J. A. Spencer, M. Yu, A. Pely, A. Engstrom and H. Zhu, *Cell*, 2014, **158**, 1110-1122.
26. S. Riethdorf, H. Fritsche, V. M uller, T. Rau, C. Schindlbeck, B. Rack, W. Janni, C. Coith, K. Beck and F. J anicke, *Clinical Cancer Research*, 2007, **13**, 920-928.
27. M. Yu, A. Bardia, B. S. Wittner, S. L. Stott, M. E. Smas, D. T. Ting, S. J. Isakoff, J. C. Ciciliano, M. N. Wells and A. M. Shah, *science*, 2013, **339**, 580-584.
28. S. T. Ligthart, F. A. Coumans, F.-C. Bidard, L. H. Simkens, C. J. Punt, M. R. de Groot, G. Attard, J. S. de Bono, J.-Y. Pierga and L. W. Terstappen, *PloS one*, 2013, **8**, e67148.
29. S. Park, R. R. Ang, S. P. Duffy, J. Bazov, K. N. Chi, P. C. Black and H. Ma, *PloS one*, 2014, **9**, e85264.



Table of Contents Entry: Manuscript ID AN-ART-09-2014-001768

Title: Efficient Microfluidic Negative Enrichment of Circulating Tumor Cells in Blood using Roughened PDMS



Depletion of >99.7% WBCs enabling tumor cell recovery from blood with nano-rough PDMS microfluidic negative enrichment devices functionalised with anti-CD45.